Anomalous absorption of neutron partial waves by the nuclear optical potential

M. Kawai and Y. Iseri
Department of Physics, Kyushu University, Fukuoka 812, Japan
(Received 23 July 1984)

Anomalously strong absorption of neutron partial waves by the nuclear optical potential is investigated in detail. More than 100 cases of anomalously strong absorption are found over the entire Periodic Table of stable nuclei in the range of energy 0—80 MeV and orbital angular momentum 0—13. A study of the S matrix in the complex-k plane reveals two different types of anomalous absorption. Discussions are given on systematics of the anomaly, its wave function, its relation to the strong absorption in the heavy-ion scattering and to the so-called unstable bound states, and on the experimental observation of the anomaly, which could be a new test of the optical potential.

I. INTRODUCTION

In the course of a recent preequilibrium analysis of low energy (n,n′) reactions,[1] it was found that the S-matrix element of the elastic scattering of neutrons by standard optical potentials becomes anomalously small for certain combinations of the target nucleus, the incident energy, and the angular momentum. The modulus of the S-matrix element was found to be of the order of 10^{-2} in certain cases. Some 30 such anomalies were reported over the entire mass number region of the target nucleus in the range of the incident energy from 0 to ~40 MeV and the orbital angular momentum l up to 11.

The physical meaning of the anomaly is obvious. Vanishing of the S-matrix element implies absence of the outgoing wave in the asymptotic region. Hence, such a partial wave is completely absorbed by the potential. In general, whenever the S-matrix element gets extremely small, anomalously strong absorption of the partial wave occurs. In the following, we shall call the phenomenon anomalous absorption for short.

Strong absorption is common in the scattering of heavy ions by nuclei. There, however, the S-matrix element is always nearly equal to zero for all the partial waves up to a certain angular momentum. In contrast, anomalous absorption in neutron scattering occurs only for special combinations of the target nucleus, energy, and angular momentum. This suggests that the two kinds of strong absorption are of different origins. We shall see in the subsequent sections that this is indeed the case.

In the present paper, we report on a detailed investigation of anomalous absorption of neutron partial waves by the optical potential of Becchetti and Greenlees.[2] We have made a similar survey as in Ref. 1, but in greater detail and with much greater precision. We have investigated the nature of anomalous absorption by studying the S matrix on the complex-k plane. We found in particular that one can discern two different types of anomalous absorption. We have also studied systematics of the anomaly, its wave function, and its relation to the strong absorption of heavy ions in the optical potential and also to the so-called unstable bound state.

In Sec. II the result of the survey is presented. In Sec.

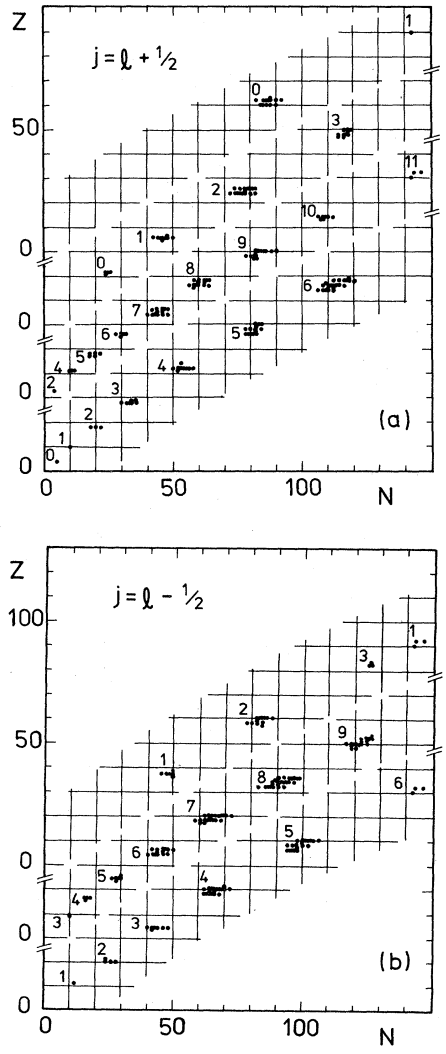

FIG. 1. Distribution of anomalous absorption on the (N,Z) plane of target nuclides. Anomalies with $j=l+\frac{1}{2}$ and $j=l-\frac{1}{2}$ are plotted separately in (a) and (b), respectively, each labeled by its l value. They are classified into series, each with consecutive l and plotted on different ordinates.

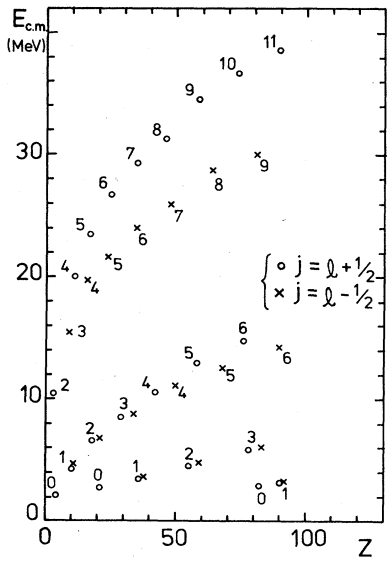

FIG. 2. Distribution of anomalous absorption on the (Z,E) plane. Circles are for $j=l+\frac{1}{2}$ and crosses are for $j=l-\frac{1}{2}$. The numbers indicate the l of the anomaly.

III discussions are given on the aspects of the anomaly already mentioned. A discussion is also given on some conditions for experimental observation of the anomaly. In Sec. IV, a summary is given. A method of solving the one-body Schrödinger equation for complex values of k is described in the Appendix.

II. NUMERICAL RESULTS

We have made the survey over all the stable nuclei (lifetime $\geq 5\times 10^8$ yr) and the range of center-of-mass energy $0<E<80$ MeV, orbital angular momentum $0\leq l\leq 13$, and total angular momentum $j=l\pm\frac{1}{2}$. For each set of l, j, E, proton number Z, and neutron number N of the target nucleus, we have calculated the S-matrix element S_{lj} with the parameters of the Becchetti-Greenlees potential obtained from the formula in Ref. 2.

The result is summarized in Figs. 1—3 and in Table I. Figure 1 shows the distribution of the anomaly with $|S|$ less than 0.05 on the (N,Z) plane. The regularity of the distribution in Fig. 1 is striking. Similar regularity can also be seen in the (E,Z) and (E,l) planes as shown in Figs. 2 and 3, respectively. We discuss these regularities in Sec. III.

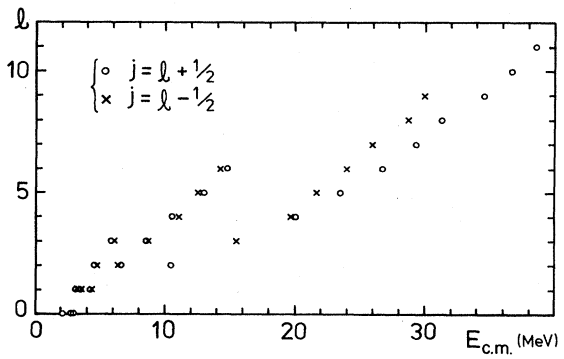

FIG. 3. Distribution of anomalous absorption on the (l,E) plane. Circles are for $j=l+\frac{1}{2}$ and crosses are for $j=l-\frac{1}{2}$.

Table I lists the minimum value of $|S|$ in each cluster of anomalies in Fig. 1. One sees that in certain cases $|S|$ is of the order of 10^{-4}, which is two orders of magnitude smaller than those found in Ref. 1. Even smaller values of $|S|$ could be attained if (N,Z) were not restricted to stable nuclei. It should be remarked in passing that the minimum value of $|S|$ is more sensitive to Z than to the mass number A in the vicinity of anomalous absorption.

III. DISCUSSIONS

In this section we discuss some salient features of anomalous absorption surveyed in Sec. II.

A. Origin of anomalous absorption

It is evident that anomalous absorption is caused by the imaginary part of the optical potential; a real potential can give only S-matrix elements of modulus unity. A very strong absorptive potential, however, does not always cause anomalous absorption. In fact, if such a potential damps the wave function to zero near the potential boundary within a distance much shorter than the wavelength, it gives rise to a strong reflected outgoing wave. This is because in such a case the wave function outside the potential behaves as if it had a node at the potential boundary. A node, however, requires the presence of an incoming wave and an outgoing wave of equal amplitudes.

Thus one sees that anomalous absorption occurs only under very special circumstances. It, therefore, seems remarkable that it occurs for the realistic neutron optical potential of Ref. 2. The question then is, what are the effects of the imaginary potential which cause anomalous absorption?

To see this, we investigate the behavior of the S-matrix element $S_{lj}(k)$ as a function of the wave number k in the complex-k plane. The Becchetti-Greenlees potential at each k is assumed to be that at the energy corresponding to $\mathrm{Re}(k^2)$. Figure 4 shows an example of the contour map of $\log_{10}|S_{lj}(k)|$ on the complex-k plane when anomalous absorption takes place. It is for the case of the neutron partial wave with $l=6$ and $j=\frac{13}{2}$ on ^{192}Os.

The figure shows that $S_{lj}(k)$ has a zero almost exactly on the real axis where the minimum value of $|S_{lj}(k)|$ is of the order of 1.3×10^{-3}, almost complete absorption. An interesting feature of Fig. 4 is the presence of a pole at $k=(0.65,-0.18)$. It turns out that this pole is very relevant to the discussion of the origin of the zero in question.

One can see this if one varies the strength of the imaginary potential by varying a multiplicative factor N_I to observe the resulting change in the pattern of the contour map, especially the movement of poles and zeros. Actually, this type of investigation has been reported in Refs. 3

TABLE I. Summary of the minimum values of $|S|$ in each cluster of points in Fig. 1. The $\pm$ correspond to $j=l\pm\frac{1}{2}$. The numbers in the parentheses represent minus the power of 10 by which the preceding number is multiplied. The A and R in the last column stand for the anti-bound-state-pole and resonance-pole origin, respectively, of the anomaly discussed in Sec. III.

l	($\pm$)	A	Z	N	k (fm^{-1})	$E_{\text{c.m.}}$ (MeV)	$\lvert S\rvert$	Origin
0	(+)	9	4	5	0.303	2.117	1.096(2)	A
		45	21	24	0.358	2.718	2.277(2)	A
		144	62	82	0.371	2.876	4.077(3)	A
1	(+)	20	10	10	0.442	4.256	4.395(2)	R
		83	36	47	0.405	3.444	8.984(4)	R
		232	90	142	0.386	3.105	2.158(2)	R
1	(−)	23	11	12	0.450	4.384	2.714(3)	R
		88	38	50	0.414	3.597	4.395(3)	R
		235	92	143	0.397	3.284	9.865(4)	R
2	(+)	7	3	4	0.664	10.455	2.982(2)	R
		36	18	18	0.556	6.592	8.560(4)	R
		133	55	78	0.466	4.539	4.805(3)	R
2	(−)	45	21	24	0.549	6.393	8.769(3)	R
		141	59	82	0.479	4.794	2.185(3)	R
3	(+)	63	29	34	0.635	8.499	1.058(2)	R
		195	78	117	0.528	5.814	8.363(4)	R
3	(−)	19	9	10	0.842	15.484	8.197(4)	R
		74	34	40	0.646	8.776	2.258(3)	R
		209	83	126	0.540	6.079	2.505(2)	R
4	(+)	23	11	12	0.962	20.036	1.145(2)	R
		98	42	56	0.710	10.566	1.354(3)	R
4	(−)	32	16	16	0.960	19.719	1.757(2)	R
		112	50	62	0.728	11.094	1.031(3)	R
5	(+)	37	17	20	1.050	23.493	2.126(2)	R
		138	58	80	0.788	12.977	2.069(3)	R
5	(−)	54	24	30	1.013	21.686	8.007(3)	R
		168	68	100	0.776	12.568	1.135(3)	R
6	(+)	55	25	30	1.125	26.737	1.377(2)	R
		192	76	116	0.842	14.786	1.329(3)	R
6	(−)	81	35	46	1.069	24.003	1.591(3)	R
		232	90	142	0.827	14.252	9.685(3)	R
7	(+)	79	35	44	1.181	29.305	2.529(3)	R
7	(−)	116	48	68	1.113	25.924	1.019(3)	R
8	(+)	110	46	64	1.223	31.316	1.338(3)	R
8	(−)	152	164	88	1.173	28.736	2.227(3)	R
9	(+)	141	59	82	1.286	34.557	6.858(3)	R
9	(−)	205	81	124	1.199	29.973	2.763(3)	R
10	(+)	182	74	108	1.327	36.737	8.788(4)	R
11	(+)	232	90	142	1.361	38.598	1.345(3)	R

and 4 with some numerical examples for square well potentials. Although those works do not cover the whole range of situations in the present analysis, they are useful as references in the numerical works described in the following.

Before going into detailed discussions of the numerical results, it is useful to remember some general analytical properties of the S-matrix element for scattering by a complex potential. These may be summarized as follows.[3,4]

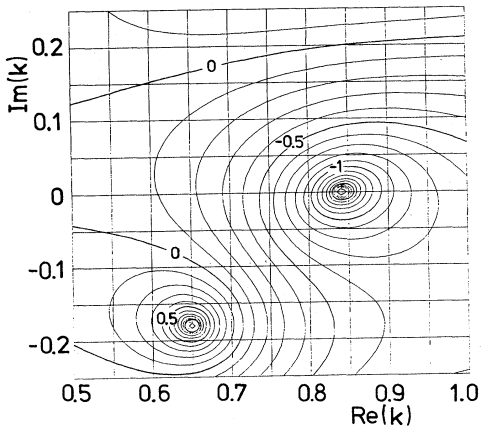

FIG. 4. Contour map of $\log_{10}|S|$ on the complex-k plane in the case of $l=6$ and $j=\frac{13}{2}$ on ^{192}Os for which anomalous absorption occurs.

If one denotes the S-matrix element for a complex potential V by $S_{lj}(k,V)$:

(a) $S_{lj}(k,V)$ and its counterpart for the complex conjugate potential V^* are related to each other through

$$S_{lj}(k,V)S^*_{lj}(k^*,V^*)=1\ . \tag{1}$$

In particular, if V is real,

$$S_{lj}(k,V)S^*_{lj}(k^*,V)=1\ . \tag{2}$$

(b) For any V, $S_{lj}(k,V)$ is related to its value at $-k$ through

$$S_{lj}(k,V)S_{lj}(-k,V)=1\ . \tag{3}$$

(c) If V is a nonregenerative potential, i.e., $\mathrm{Im}(V)\leq 0$, $S(k,V)$ is regular in the first quadrant of the complex-k plane.

These properties can be readily derived from the Schrödinger equation and the boundary condition imposed on the wave function.[4]

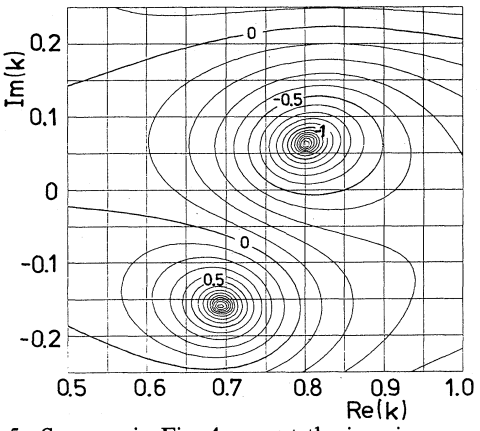

FIG. 5. Same as in Fig. 4, except the imaginary potential is reduced by a factor $N_I=0.5$.

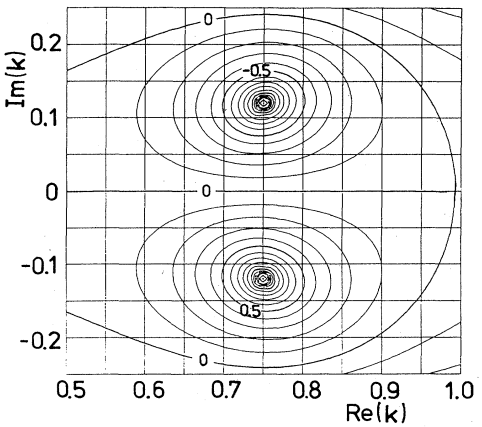

FIG. 6. Same as in Fig. 4, except $N_I=0.0$, i.e., the potential is real.

Figures 5 and 6 show the contour maps corresponding to Fig. 4 but for $N_I=0.5$ and 0.0, respectively. At $N_I=0.0$, i.e., when the potential is real, a zero and a pole of the S-matrix element are located at the positions symmetric with respect to the real axis. This is because of Eq. (2); a pole in the fourth quadrant, a decaying-state-resonance pole, necessitates a zero in the first quadrant at a complex-conjugate position.

For $N_I\neq 0$, Eq. (2) does not hold any more, nor does the symmetry of the pole and the zero with respect to the real axis. Figures 4 and 5 show, however, that the zero and the pole move as a correlated pair when N_I changes. As N_I increases, the pattern of the contour map rotates clockwise, the pole and the zero both moving downwards. This is because the pole cannot move upward into the first quadrant because of property (c). It actually moves away from it in this particular case, in agreement with the cases investigated in Ref. 4. Correlated to this movement of the pole, the zero moves down and almost exactly reaches the real axis at $N_I=1.0$, resulting in Fig. 4. The movement of the zero is depicted in Fig. 7 by curve (1).

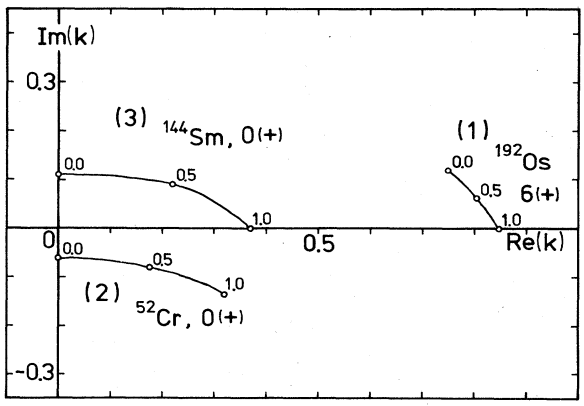

FIG. 7. Loci of the zero for varying strength of the imaginary potential. They are associated with a resonance pole [curve (1)], a bound-state pole [curve (2)], and an anti-bound-state pole [curve (3)], corresponding to Fig. 4, the $l=0$, $j=\frac{1}{2}$ wave on ^{52}Cr, and Fig. 8, respectively. The numbers attached to the circles indicate the values of N_I.

The foregoing analysis suggests that there may be other types of anomalous absorption, depending on the kind of pole with which the zero is associated. There are two types of poles of the S-matrix element other than the resonance pole. For a real potential, one is the bound-state pole on the positive imaginary axis and the other is the anti-bound-state pole on the negative imaginary axis. A zero is associated to each of these poles according to Eq. (3) which dictates that if a pole is at $k=k_0$, there must be a zero at $k=-k_0$. On the complex-k plane they are symmetric to each other with respect to the origin.

This symmetry is maintained even when an absorptive potential is introduced and the poles move away from the imaginary axis as the strength of the imaginary potential is increased. In the particular cases investigated here the movement of the pole-zero pair turns out to be as follows.

A bound-state pole must move to the left from the imaginary axis into the second quadrant, again because of property (c). The zero associated with it, therefore, moves to the right from the negative imaginary axis into the fourth quadrant. Its vertical movement, however, turns out to be either downward or only slightly upward. An example is shown in Fig. 7, curve (2). Even at the full strength of the imaginary potential, the zero does not approach the real axis close enough to cause a significant absorption. Thus, there is no anomalous absorption associated with a bound-state pole for the Becchetti-Greenlees potential in the energy range considered here.

There is no restriction of movement for anti-bound-state poles such as the one for bound-state poles. It turns out, however, that in the particular cases investigated here their movement is such that the associated zeros move from the imaginary axis to the right and downward, sometimes getting very close to the real axis at the full strength of the imaginary potential. An example is shown in Fig. 7, curve (3), for the case of the $l=0$, $j=\frac{1}{2}$ wave on ^{144}Sm. The corresponding contour map of $\log_{10}|S|$ at $N_I=1.0$ is shown in Fig. 8. One indeed sees a zero very close to the real axis, but no associated resonance pole in the fourth quadrant, in contrast to Fig. 4. The latter feature is in fact a signature of the anti-bound-state-pole origin of the anomaly.

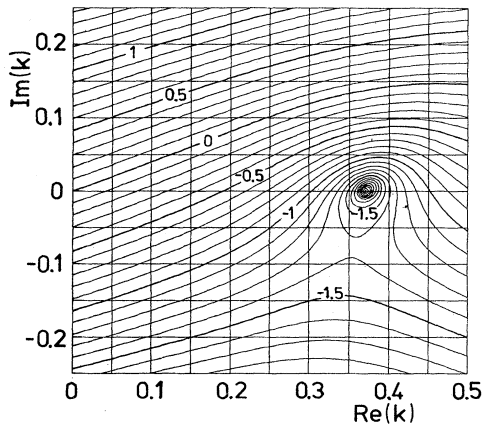

FIG. 8. Contour map of $\log_{10}|S|$ for the case of $l=0$, $j=\frac{1}{2}$ on ^{144}Sm.

Anomalous absorption of this type has been found only for $l=0$ among the cases studied here. All the other anomalies are associated with a resonance pole.

B. Regularity in the distribution of the anomaly

In Sec. II A we saw in different kinds of representations in Figs. 1–3 that the distribution of anomalous absorption is quite regular. In each of those figures, the points cluster into eight groups, each of which, except for the isolated two, forms a smooth line with the consecutive l's. A similar pattern can also be seen in the distribution of the anomaly on the (l,A) plane.

The regularity is perhaps not so surprising if one considers the condition for anomalous absorption

$$u'_{lj}(k,r)/u_{lj}(k,r)\,|_{r=R} = [rh_l^{(-)}(kr)]'/[rh_l^{(-)}(kr)]\,|_{r=R}\ , \quad (4)$$

where $u_{lj}(k,r)$ is r times the radial wave function of the partial wave (l,j), $h_l^{(-)}(x)$ is the spherical Hankel function of the second kind, i.e., an incoming free wave, and R is an arbitrary point in the asymptotic region. Equation (4) governs the relationship among the values of E, Z, N, and l at the anomaly. Since potential parameters and the functions in Eq. (4) depend smoothly on E, Z, and N and change systematically with l and j, one would expect some kind of a systematic pattern in diagrams like Figs. 1–3. Conversely, the patterns in those figures indicate some simple relationship between the values of the parameters at the anomaly. The relationship is even more clearly revealed by a plot on the $(l/k, A^{1/3})$ plane as shown in Fig. 9. One sees that again the points cluster into eight groups. However, except for the low l's, for all the six groups already mentioned the lines connecting the points are very nearly straight. An analytic expression for the straight lines is

$$l/k = r_1 A^{1/3} + \delta\ , \quad (5)$$

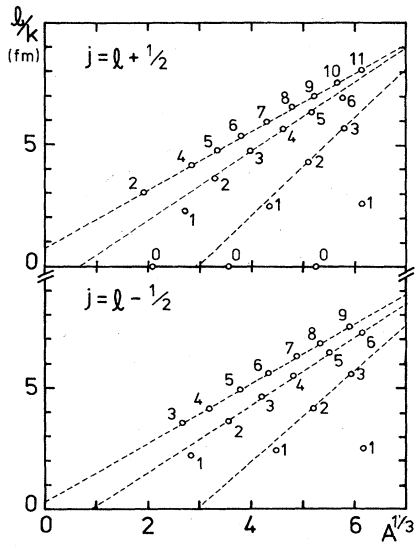

FIG. 9. Distribution of anomalous absorption on the $(l/k, A^{1/3})$ plane. The numbers indicate the l of the anomaly.

where r_1 and δ are constants. For the six curves (r_1,δ) equals (1.20, 0.76), (1.42, −1.00), and (1.99, −5.84), respectively, for $j=l+\frac{1}{2}$ and (1.22, 0.30), (1.40, −1.27), and (1.89, −5.65), respectively, for $j=l-\frac{1}{2}$. One cannot draw meaningful straight lines through the points of the other two groups.

The analysis described above is related to a previous attempt of Haruta[5] to deduce the "radius parameter," r_2, from the relations $l=kR$ and $R=r_2A^{1/3}$, where l and k are those at anomalous absorption. He obtained for some 16 anomalies the value of r_2 ranging from 1.35 to 1.43 for $j=l+\frac{1}{2}$ and from 1.19 to 1.26 for $j=l-\frac{1}{2}$, both decreasing with increasing l. It is easy to see that this result can be explained by the linear relationship already described. We have already seen, however, that there are actually several series distinguished by different common values of r_1 and δ.

Another point to be noticed is that the values of r_1 are much larger than the radius parameter of the Becchetti-Greenlees potential, $r_0=1.17$ fm. This suggests that the two parameters are not directly related to each other and the relationship between r_0 and r_1 is rather involved.

Finally, a natural association of Fig. 3 might be with a Regge trajectory. In fact, if the potentials were real the zeros and the poles would coincide on the (E,l) plane, according to Eq. (2). Figure 3 would then be just a representation of Regge trajectories. Even for complex potentials it then seems natural to expect some strong correlation between Fig. 3 and the Regge trajectory. The derivation of an explicit relationship between the two, however, does not seem simple.

C. Wave function at anomaly

In order to see what happens to the wave function when anomalous absorption occurs, we plotted $u_{lj}(k,r)$ as a function of r by a solid line in Fig. 10 for the case of the $l=4$, $j=\frac{7}{2}$ wave on ^{112}Sn at 11.094 MeV. For comparison, the same wave function at neighboring energies is also plotted in Fig. 10. One sees that the wave functions are almost the same inside the potential and the average modulus of the amplitudes outside the potential is also essentially the same. The only qualitative dependence on E is that at the anomaly there is an absence of oscillation in the asymptotic region, due to the lack of the outgoing wave.

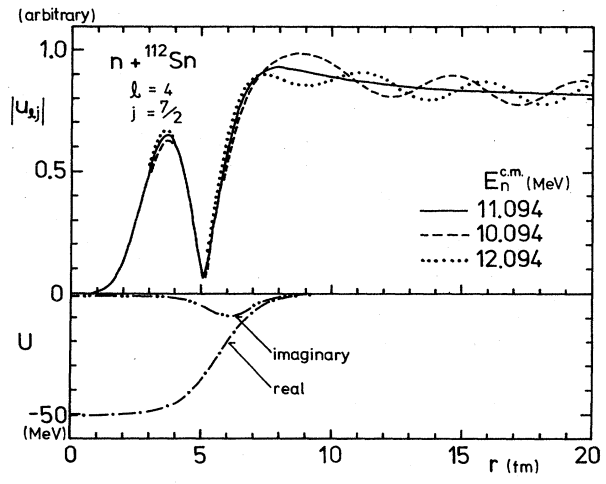

FIG. 10. The radial function $u_{lj}(k,r)$ for $l=4$, $j=\frac{7}{2}$ on ^{112}Sn as a function of r when anomalous absorption occurs at 11.094 MeV (solid line) and when the energy is off the anomaly by −1 MeV (broken line) and + 1 MeV (dotted line), respectively.

The features of the wave function already described are in sharp contrast to the resonance enhancement of a wave function inside the potential. The difference between the two cases can be understood qualitatively in terms of Jost's wave functions $f_{lj}^{(\pm)}(k,r)$, defined by the asymptotic boundary conditions

$$\lim_{r\to\infty} e^{\mp ikr} f_{lj}^{(\pm)}(k,r)=1\ , \tag{6}$$

if one writes $u_{lj}(k,r)$ in the form

$$u_{lj}(k,r)=f_{lj}^{(-)}(k,r)-S_{lj}(k)f_{lj}^{(+)}(k,r)\ . \tag{7}$$

Near a resonance, S_{ij} becomes very large, indicating some anomalous behavior of $u_{lj}(k,r)$ inside the potential. At a zero of S_{ij}, however, $u_{lj}(k,r)$ simply reduces to $f_{lj}^{(-)}(k,r)$ and is not drastically different from the wave function at neighboring energies inside the potential. This is the reason why nothing spectacular is seen in Fig. 10 except for the monotonic modulus of the amplitude in the asymptotic region. Furthermore, the transition from the oscillating to the monotonic modulus is rather gradual, being over the "width" of the zero, of the order of an MeV as one can see, for example, in Fig. 4.

D. Comparison with absorption in heavy-ion scattering

Let us compare anomalous absorption discussed so far with the strong absorption of heavy ions by complex optical potentials. In the case of heavy ions, all the low par-

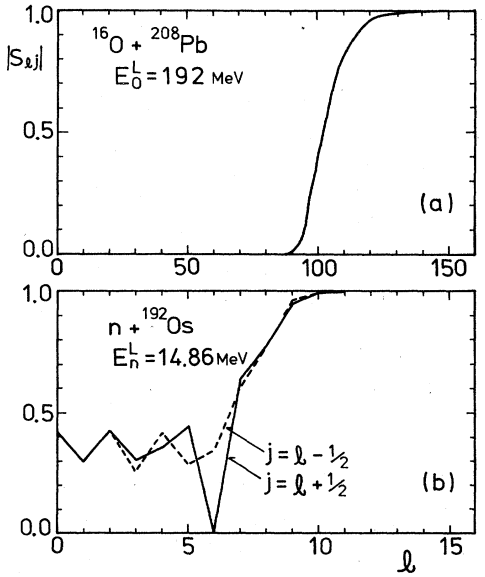

FIG. 11. $|S|$ as a function of l in the case of (a) a heavy-ion scattering, ^{16}O on ^{208}Pb at $E_{\rm lab}=192$ MeV, after Ref. 6, and (b) a neutron scattering on ^{192}Os at $E_{\rm lab}=14.86$ MeV.

tial waves up to a certain angular momentum are almost completely absorbed by the absorptive potential. An example is shown in Fig. 11(a).[6] This is in contrast to the case of neutrons in which anomalous absorption occurs only in one particular partial wave, as shown in Fig. 11(b), for special combinations of the energy and target nucleus.

A basic theoretical difference between the two cases is that one can use a semiclassical analysis reasonably well for the heavy-ion scattering but not for the neutron scattering considered here. Thus, the strong absorption in the heavy-ion scattering can be attributed to the strong absorption of the flux by the complex potential in the course of the wave coming from infinity, getting into the potential, propagating inward, bounced back by the centrifugal barrier, or at the origin if it is an s wave, and propagating outward, eventually out of the potential. The longer the distance the wave has to travel inside the potential, the more flux is absorbed. In turn, the lower the angular momentum of the partial wave, the longer the distance it has to travel. If the absorptive potential is sufficiently strong, as in the case of actual heavy-ion scattering, all the low partial waves up to a certain angular momentum are almost completely absorbed, resulting in extremely small S-matrix elements.

The preceding arguments are based on the lowest order Wentzel-Kramers-Brillouin (WKB) approximation which is valid if the potential varies slowly, changing little within a distance of the local wavelength. This, in fact, is a reasonable zeroth order assumption for the heavy-ion scattering by the optical potential.

The approximation, however, is not well justified for neutron scattering by the optical potential at energies less than 40 MeV. The wavelength is large and the change of the potential within that distance is appreciable in the surface region. In such a case, the gradient of the potential causes a reflection of the wave function. In particular, the incident wave is partly reflected back on the slope of the potential, causing outgoing waves. This obviously invalidates the lowest order description already given but is what actually happens in the neutron scattering considered here. Anomalous absorption in this case is the result of mutual cancellation of outgoing waves generated at different regions in the potential. This can happen only under special circumstances with special combinations of energy, angular momentum, and potential. Thus, it differs from the strong absorption of heavy ions in its origin as well as in its apparent features.

E. Relation to "unstable bound state"

If a zero that causes anomalous absorption is slightly below the real axis in the complex-k plane, a pole exists in the second quadrant slightly above the real axis, according to Eq. (3). The wave number at the pole has a small positive imaginary part. The wave function, therefore, decays exponentially at infinity, representing a bound state. Although the complex energy eigenvalue makes the bound state unstable, its small imaginary part makes the width of the state narrow. Poles of this nature have been considered as an interpretation of some Σ-nuclear states with extremely narrow widths[7,8] and called unstable bound states. Present analysis shows that such poles actually exist in some neutron-nucleus systems. It is, however, clear that the existence is rather fortuitous, depending critically on the strength of the imaginary potential; for a slightly weaker imaginary potential the pole would correspond to an unbound state. Another problem is whether or not an unstable bound state is of real physical significance. One might argue that the negative real part of the wave number indicates that the pole does not correspond to any physically realizable state. We shall not discuss this problem any further here because the subject is obviously beyond the scope of the present paper.

F. Experimental observation

It would be extremely interesting if anomalous absorption of neutron partial waves could be observed by experiments. The question is whether and how it could be done. This is not a trivial question, because anomalous absorption occurs only in one partial wave at an energy, and it reduces, rather than enhances, its outgoing wave amplitude. Hence, it will be difficult to detect it in any physical quantity that involves many partial waves. One will have to look for an experiment that somehow picks out individual partial waves, in particular the one that is absorbed anomalously. Another point is that the S-matrix element varies rather slowly across the anomaly as already mentioned. One has to look for an anomaly that extends over an energy range of the order of an MeV. Whether an experiment satisfying these conditions is actually feasible is a very interesting open question.

IV. SUMMARY AND CONCLUSION

Anomalous absorption of neutron partial waves by nuclei has been investigated with the optical potential of Becchetti and Greenlees for the stable target nuclides over the entire Periodic Table. The anomaly is found in more than 100 cases in the range of angular momentum from 0 to 13 and of energy from 0 to 80 MeV. The anomaly is investigated in detail through a study of the S-matrix element on the complex-k plane. The origin of anomalous absorption is identified to be a zero conjugate to a pole of the S-matrix element, moved to a point close to the positive real axis by the imaginary part of the optical potential. One can distinguish two types of anomalous absorption, depending on the kind of pole with which the zero is associated. Among the three types of poles of the S matrix, i.e., the decaying-state-resonance pole, the antibound-state pole, and the bound-state pole, the first two have an associated anomalous absorption, while the bound-state pole happens to have none, at least not in the particular cases investigated.

Regularity is seen in the distribution of the anomaly on the (Z,E), (l,E), and $(l/k,A^{1/3})$ planes. The points representing the anomaly on those planes cluster into eight groups, each consisting of one, two, or more than three points. Each of the six last groups form a smooth line with the points of consecutive l values on it. Especially, the lines on the $(l/k,A^{1/3})$ plane are nearly straight except for the low l's. The constants r_1 and δ in the equation $l/k = r_1 A^{1/3} + \delta$ representing the straight line

are extracted by the method of least squares. The values of r_1 are found to be considerably larger than the radius parameters r_0 of the Becchetti-Greenlees potential.

A wave function which suffers anomalous absorption shows no anomaly inside the potential. This is because of the presence of the $f_{lj}^{(-)}$ component in the wave function which survives anomalous absorption. The only visible anomaly is the monotonic modulus of the amplitude in the external region due to the lack of the outgoing wave.

Anomalous absorption in the neutron scattering is compared with the strong absorption of low partial waves in the heavy-ion scattering. A qualitative difference between the two cases is that the former occurs only for special combinations of target nucleus, angular momentum, and energy, while the latter occurs always and in all partial waves up to a certain angular momentum. The difference is attributed to the presence or virtual absence of the reflected waves generated by the gradient of the potential in the surface region, due to the difference between the two cases in the wavelength relative to the diffuseness of the potential.

There are cases in which a zero is just below the positive real axis. The pole conjugate to such a zero is slightly above the negative real axis and it corresponds to a so-called unstable bound state. Existence of such a pole, however, depends very sensitively on the strength of the imaginary potential. Its real physical significance is not yet established either.

Another open question is whether anomalous absorption is experimentally observable. If it is, it will probably be in an observation which picks out individual partial waves, in particular the one anomalously absorbed, over an energy range of the order of an MeV. Such an experiment, if feasible, would be a new test of the optical potential because anomalous absorption depends on the optical potential in a different manner from quantities hitherto observed.

Finally, it seems natural to assume that anomalous absorption is not restricted to neutron scattering. In fact, a preliminary calculation shows it occurs also in proton scattering. Possibly, it occurs in the scattering of light composite particles as well. It will be very interesting to see how universal the phenomenon is in the entire realm of the nuclear scattering of light ions.

ACKNOWLEDGMENTS

The authors wish to thank Professor I. Kumabe for his communications about Ref. 1 and Mr. H. Haruta for his providing them with detailed information on his thesis work of Ref. 5. The kind help of Professor N. Austern in preparing the manuscript is also gratefully acknowledged. The authors are also much indebted to Professor Y. Fukushima for his help in numerical computations. The computations were done at the Computing Center of Kyushu University with the computer FACOM-M382, with the financial support of the Institute for Nuclear Study, University of Tokyo.

APPENDIX

The Schrödinger equation for r times the radial wave function $u \equiv u_{lj}(k,r)$ for a partial wave (l,j) reads

$$u''+(k^2-U)u=0\ , \tag{A1}$$

where $U=(2\mu/\hbar^2)V+l(l+1)/r^2$, μ being the neutron reduced mass. The asymptotic boundary condition for u is

$$u\sim u^{(-)}-Su^{(+)}\ , \tag{A2}$$

where $u^{(\pm)}=rh_l^{(\pm)}$ are the outgoing and incoming waves, respectively, with the asymptotic forms

$$u^{(\pm)}\sim\exp[\pm i(kr-l\pi/2)]\ . \tag{A3}$$

If k is complex, one of the $u^{(\pm)}$ grows exponentially as r increases in the asymptotic region, and so does u. This causes difficulty if one tries to solve Eq. (A1) in the usual way with a step-by-step method from $r=0$ to a point $r=r_{\max}$ in the asymptotic region. In this appendix we describe a method of circumventing this difficulty.

For this purpose, we divide the r space into three regions: (1) $0\le r\le r_0$, (2) $r_0\le r\le r_{\max}$, and (3) $r_{\max}\le r$, defined in the following way. In region (1), one can solve Eq. (A1) by a step-by-step method from $r=0$ to $r=r_0$ and get a solution $u=u_1$ without the difficulty of exponential growth of u. Region (3) is the asymptotic region where the solution $u=u_3$ has the form of Eq. (A2),

$$u_3=u^{(-)}-Su^{(+)}\ . \tag{A4}$$

It is in region (2) in which one has to take care of the exponential growth of u.

In region (2), one introduces an auxiliary function w by

$$w=u-u^{(-)} \tag{A5}$$

if $\mathrm{Im}(k)\ge 0$. The function w is well behaved in region (2) and it satisfies the asymptotic boundary condition

$$w\sim -Su^{(+)}\ , \tag{A6}$$

which follows from Eqs. (A2) and (A5). The equation for w is obtained from Eqs. (A1) and (A5) as

$$w''+(k^2-U)w=Uu^{(-)}\ . \tag{A7}$$

The general solution of Eq. (A7) is of the form

$$w=\alpha w_H+w_I\ , \tag{A8}$$

where α is an arbitrary constant, w_H is a general solution of the homogeneous equation

$$w_H''+(k^2-U)w_H=0\ , \tag{A9}$$

and w_I is a particular solution of the inhomogeneous equation, (A7),

$$w_I''+(k^2-U)w_I=Uu^{(-)}\ . \tag{A10}$$

We choose w_H and w_I such that they satisfy the asymptotic boundary conditions

$$w_H\sim au^{(+)}$$

and (A11)

$$w_I\sim bu^{(+)}\ ,$$

where a and b are appropriately chosen constants. In order for this to be possible for w_I, it is necessary that the

right-hand side of Eq. (A10) be negligibly small compared with the left-hand side for sufficiently large r. If U changes asymptotically as $e^{-r/m}$, this requires

$$2\,\mathrm{Im}(k) < 1/m \ . \tag{A12}$$

We, therefore, restrict ourselves to the value of k which satisfies (A12). The solution $u = u_2$ in region (2) thus obtained is given, from Eqs. (A5) and (A8), by

$$u_2 = u^{(-)} + (\alpha w_H + w_I) \ . \tag{A13}$$

The solution is smoothly connected to u_1 at r_0 and to u_3 at $r_{\max}$. The first condition gives

$$u_2'(r_0)/u_2(r_0) = u_1'(r_0)/u_1(r_0) \equiv \gamma \tag{A14}$$

from which α is determined as

$$\alpha = [u^{(-)'} + w_I' - \gamma(u^{(-)} + w_I)]/(\gamma w_H - w_H') \ . \tag{A15}$$

The condition at $r = r_{\max}$ is satisfied if, according to Eqs. (A4), (A11), and (A13),

$$S = -(\alpha a + b) \ . \tag{A16}$$

Equation (A16) together with Eq. (A15) determines S.

[1]M. Haruta, M. Hyakutake, M. Matoba, and I. Kumabe, Phys. Lett. **140B**, 272 (1984).
[2]F. D. Becchetti, Jr. and G. W. Greenlees, Phys. Rev. **182**, 1190 (1969).
[3]S. Joffily, Nucl. Phys. **A215**, 301 (1973).
[4]W. Cassing, M. Stingl, and A. Weiguny, Phys. Rev. C **26**, 22 (1982).
[5]M. Haruta, Masters thesis, Kyushu University, 1983.
[6]J. B. Ball, C. B. Fulmer, E. E. Gross, M. L. Halbert, D. C. Hensley, C. A. Ludermann, M. J. Saltmarsh, and G. R. Satchler, Nucl. Phys. **A252**, 208 (1975).
[7]A. Gal, G. Toker, and Y. Alexander, Ann. Phys. (N.Y.) **137**, 341 (1981).
[8]C. J. Batty, A. Gal, and G. Toker, Nucl. Phys. **A402**, 349 (1983). See also R. Shanta, Nucl. Phys. **A199**, 624 (1973).